

# Instabilities in the asymptotic suction boundary layer over a permeable, compliant wall

Franck Pluvinage,<sup>1,a)</sup> Azeddine Kourta,<sup>1</sup> and Alessandro Bottaro<sup>2</sup>

<sup>1</sup>University of Orléans, INSA-CVL, PRISME, EA 4229, F45072 Orléans, France

<sup>2</sup>DICCA, Scuola Politecnica, Università di Genova, 1 via Montallegro, 16145 Genova, Italy

(Received 22 December 2014; accepted 6 May 2015; published online 22 May 2015)

The spatial, linear stability of an incompressible parallel boundary layer flow with uniform suction through the wall is studied for the case of rigid and flexible bounding surfaces. It is demonstrated, first, that the effect of the plate's permeability is crucial in defining the disturbance boundary conditions at the wall, and that stability limits depend strongly on it. Next, the combined effect of plate's permeability and compliance on the onset of Tollmien-Schlichting modes is assessed. Finally, the possible insurgence of an absolute instability mode is studied, as function of the Reynolds number, the modulus of elasticity of the plate, and its permeability. © 2015 AIP Publishing LLC. [<http://dx.doi.org/10.1063/1.4921422>]

## I. INTRODUCTION

Laminar flow control, via boundary layer suction, is a well-known technique to increase aerodynamic performances. This method is suitable to delay laminar-turbulent transition<sup>1</sup> but is not effective if the objective is that of relaminarizing a turbulent flow because of the high input energy needed to apply adequate suction speeds.

The present work deals with the initial stages of the transition process taking place on a flat plate boundary layer, with suction applied through the surface. The study is restricted to the special case of the asymptotic suction boundary layer, whose threshold for transition has long been believed to be around the exceptionally high displacement-thickness-based Reynolds number of 54 000 (see, for example, the early work by Hocking<sup>2</sup> or the more recent results by Fransson and Alfredsson<sup>3</sup>), about two orders of magnitude larger than for the Blasius boundary layer at the same outer speed. Previous work on drag reduction via suction through spanwise slots, porous panels, and discrete holes has been carried out by, e.g., Pfenninger and Groth,<sup>4</sup> Reynolds and Saric,<sup>5</sup> and MacManus and Eaton.<sup>6</sup> A general review of various types of surface and of the results achieved in wind tunnel tests is given by Gregory,<sup>7</sup> where a discussion for practical applications on aircrafts is provided. MacManus and Eaton<sup>6</sup> performed both experimental and computational investigations to show that suction may destabilize the flow by introducing co-rotating streamwise vortices when discrete holes are used. In their work, the ratio of the perforation diameter to the boundary layer displacement thickness was quite large, around unity. Better control authority can be achieved by using suction panels through which a quasi-uniform normal-to-the-wall velocity distribution can be achieved. An experimental and theoretical study on the effect of boundary layer suction on the laminar-turbulent transition process has been carried out by Fransson.<sup>8</sup> In his study, an asymptotic suction boundary layer was established in a wind tunnel. Uniform suction was applied over a large area, with boundary layer thickness nearly constant over a length of 1800 mm. Fransson's linear stability results were not in close agreement with the experimental measurements, a fact which we will address in the present paper.

Aeroelastic effects are also of importance for aeronautical applications, and the interplay between suction at the wall and the plate's flexibility might be important in defining the onset of hydrodynamic instabilities. The only work to-date which has considered a bounding surface which

---

<sup>a)</sup>Electronic mail: [franck.pluvinage@univ-orleans.fr](mailto:franck.pluvinage@univ-orleans.fr)

is both compliant and (weakly) porous is due to Pluvinage *et al.*<sup>9</sup> They have treated, with the parallel flow approximation, the temporal growth of hydrodynamic and hydroelastic modes occurring in the Falkner-Skan-Cooke boundary layer. The main conclusion of their work is that the porous wall has a destabilizing influence on Tollmien-Schlichting (TS) modes, which can be mitigated by wall compliance. Porosity was found to have a stabilizing influence on flow-induced surface instabilities, such as the so-called *travelling wave flutter* (cf. Carpenter and Garrad<sup>10</sup>). As far as absolute instability modes are concerned, Lingwood<sup>11</sup> has shown that suction is capable of delaying the onset of the instabilities which can arise in the boundary layer over a rotating disk.

The linear stability analysis described in the present contribution is spatial, rather than temporal; after showing that the plate's permeability can have a profound influence on the Tollmien-Schlichting waves in the boundary layer which forms over a rigid wall, we will demonstrate that an absolute instability can arise in the boundary layer over a poroelastic plate, via the coalescence between hydrodynamic and wall-based modes.

## II. THE MODEL

### A. The asymptotic suction boundary layer (ASBL) velocity profile

The fully developed velocity profiles which set in when a fluid (of density  $\rho$  and kinematic viscosity  $\nu$ ) flows over a porous surface with a constant suction velocity  $V_o$  through the pores of the plate are<sup>12</sup>

$$U = U_\infty(1 - e^{-\frac{V_o y}{\nu}}), \quad V = V_o, \quad (1)$$

with  $U_\infty$  the external velocity parallel to the plate and  $y$  the wall-normal coordinate. Note that  $V_o$  is negative-definite for physical solutions to arise. This fully developed velocity profile is known as the ASBL; its displacement thickness  $\delta^*$  is equal to

$$\delta^* = \int_0^\infty \left(1 - \frac{U}{U_\infty}\right) dy = -\frac{\nu}{V_o}, \quad (2)$$

and the Reynolds number based on this value is  $Re = \frac{U_\infty \delta^*}{\nu} = -\frac{U_\infty}{V_o}$ . The velocity profile near the wall is fuller than in the Blasius case and — because of this — the flow is believed to be less prone to destabilization (as it occurs for the case of the boundary layer under a negative pressure gradient), as argued in a number of linear and nonlinear analyses.<sup>2,3</sup> All studies to date have consistently assumed a zero normal-to-the-wall velocity condition at the porous boundary, on the argument that a small permeability has a negligible effect on the perturbation. Such an argument is however fallacious, even for low permeabilities, as will be demonstrated herein.

### B. Linearized Navier-Stokes equations

For low environmental disturbances, transition in a flat-plate boundary layer is dominated by TS waves, which grow exponentially.<sup>3</sup> According to Squire's theorem, the critical Reynolds number is obtained for a two-dimensional wave, that is why a two-dimensional analysis will be performed here. Disturbance waves are considered of the form

$$p = \hat{p}(y) e^{i\alpha x - i\omega t}, \quad u = \hat{u}(y) e^{i\alpha x - i\omega t}, \quad v = \hat{v}(y) e^{i\alpha x - i\omega t},$$

with  $\alpha$  the streamwise wavenumber and  $\omega$  the frequency. The study focuses initially on the linear growth/decay of spatially evolving waves ( $\alpha = \alpha_r + i\alpha_i$  is thus a complex number whereas  $\omega = \omega_r + i\omega_i$  is taken with  $\omega_i$  equal to zero). In the second part of this work, Briggs' criterion<sup>13</sup> is used (i.e.,  $\omega_i$  is assigned, and a range of  $\omega_r$  is spanned) to analyze the coalescence of modes and the conditions for the occurrence of an absolute instability.

The linearized momentum and mass conservation equations in dimensionless form reduce to

$$\begin{cases} (-i\omega + i\alpha U + V_o D - \frac{\Delta}{Re})\hat{u} + (DU)\hat{v} + i\alpha\hat{p} = 0, \\ (-i\omega + i\alpha U + V_o D - \frac{\Delta}{Re})\hat{v} + D\hat{p} = 0, \end{cases} \quad (3a)$$

$$i\alpha\hat{u} + D\hat{v} = 0, \quad (3b)$$

with  $D = d/dy$  and  $\Delta = D^2 - \alpha^2$ . The equations are solved using the same Chebyshev spectral collocation method employed by Ref. 9, with  $\hat{p}$ ,  $\hat{u}$ , and  $\hat{v}$  as dependent variables. From now on, hats will be dropped from the names of the dependent variables.

### C. Boundary conditions at the wall

The boundary layer is assumed to develop above an isotropic, untensioned plate of density  $\rho_p$  and thickness  $b$ , attached to a rigid, impermeable base through regularly arranged stubs which behave like springs (cf. Fig. 1). The plate is porous, of permeability  $k_D$ , and the fluid beneath it is assumed to be maintained under controlled, unperturbed conditions. A small perpendicular displacement  $\eta^*(x, t)$  of the plate from its rest position is considered, caused by the load exerted by the medium flowing above it.

Provided that  $\eta^* \ll b$  and that the wavelength of the plate's flexural motion is much larger than  $b$ ,  $\eta^*$  satisfies the (dimensional) bending wave equation

$$\rho_p b \frac{\partial^2 \eta^*}{\partial t^{*2}} + B^* \nabla_2^4 \eta^* + \kappa^* \eta^* = -p^* \quad (4)$$

(asterisks denote dimensional variables). Accounting for both plate's deflection and flow through the pores (governed by Darcy's law), the boundary conditions for the perturbation velocity components at  $y^* = \eta^*$  are

$$u^* = 0, \quad v^* = \frac{\partial \eta^*}{\partial t^*} - \frac{k_D}{\rho_p b} p^*, \quad (5)$$

where  $k_D$  is the isotropic permeability of the plate. Once linearized, the (now dimensionless) equation for the plate's displacement becomes

$$\left( -\frac{\chi}{Re} \omega^2 - i d \omega + \frac{B}{Re^3} k^4 + \frac{T}{Re} k^2 + \kappa Re \right) \eta = -p, \quad (6)$$

and the adimensional disturbance boundary conditions at the fictitious (Kramer-type) wall placed at  $y = 0$  are

$$u + \eta U' = 0, \quad v = -i\omega\eta - ap. \quad (7)$$

Finally, the boundary conditions become

$$i \frac{\chi}{Re} \omega(v + ap) + \frac{1}{U' Re} \left( \frac{B}{Re^2} \alpha^4 + \kappa Re^2 \right) u = p, \quad (8)$$

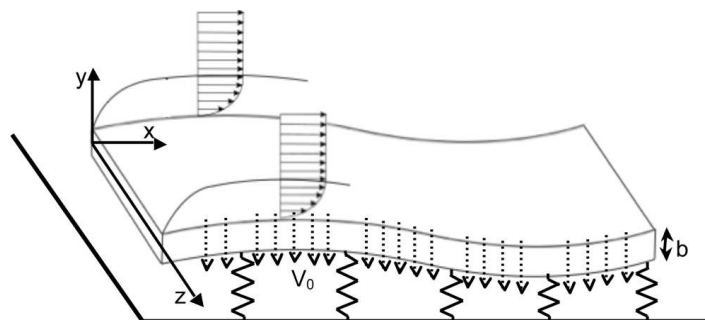


FIG. 1. Sketch of the problem considered.

$$-i\omega u + U'(v + ap) = 0, \quad (9)$$

where  $\chi = \frac{\rho_p U_\infty b}{\rho \nu}$  is the dimensionless plate mass per unit area,  $B = \frac{B^* U_\infty}{\rho \nu^3}$  the dimensionless flexural rigidity (with  $B^* = \frac{E b^3}{12(1-\nu_p^2)}$  the bending rigidity per unit width and  $\nu_p$  the Poisson ratio), and  $\kappa = \frac{\kappa^* \nu}{\rho U_\infty^3}$  the adimensional spring stiffness (the dimensional counterpart of which, per unit area, is denoted as  $\kappa^*$ ). We have used  $U_\infty$  throughout to normalise the equations; this means that the external speed is maintained constant and the Reynolds number is varied by acting on the suction velocity  $V_o$  (which must remain sufficiently smaller than  $U_\infty$  for the boundary layer equations to remain applicable); this can be easily achieved in practice by changing the mean pressure gradient across the porous plate. Furthermore, the parameter  $a$  appears in Eq. (7); it is defined as  $a = k_D U_\infty / (\nu b)$  and represents the adimensional permeability coefficient. In the rigid-plate limit, we recover  $u = v + ap = 0$  at  $y = 0$ , a condition first proposed by Gustavsson,<sup>14</sup> but never tested.

### III. COMPARISON WITH THE EXPERIMENTS BY FRANSSON AND ALFREDSSON

In order to validate the model, we compare with the wind tunnel results by Fransson and Alfredsson;<sup>3</sup> we thus consider air as the working fluid ( $\rho = 1.225 \text{ kg m}^{-3}$ ,  $\nu = 1.5 \times 10^{-5} \text{ m}^2 \text{ s}^{-1}$ ), flowing at a speed  $U_\infty = 5 \text{ m s}^{-1}$  over a  $b = 3.2 \text{ mm}$  thick porous plate, whose Young modulus is  $E = 974 \text{ MPa}$ , Poisson ratio  $\nu_p = 0.5$ , and isotropic permeability  $k_D = 3.7 \times 10^{-12} \text{ m}^2$ . By assuming a plate's density  $\rho_p = 945 \text{ kg m}^{-3}$ , the dimensionless plate mass is  $\chi = 8.23 \times 10^5$ , the flexural rigidity is  $B = 4.4 \times 10^6 E$ , and the permeability coefficient is  $a = 3.854 \times 10^{-4}$ . In the previous expression for  $B$ , the numerical value of  $E$ , in Pascal, must be inserted without its dimensional units. It is useful to write explicitly the dependence of  $B$  on  $E$ , since we will later analyze the effect of varying  $E$ .

The plate in the experiments<sup>3</sup> is sustained by longitudinal T-profiles spaced 50 mm apart from one another along the span. In the points where there is contact between the plate and the T-profile, the plate does not bend; in the space in between, the maximal deflection is measured to be around  $50 \mu\text{m}$  for a pressure difference  $\Delta P = 1500 \text{ Pa}$  across the porous plate. The value of  $50 \mu\text{m}$  agrees well with the theoretical one, which can be obtained considering a simply supported plate bent under the action of a constant pressure load. In this case, theory<sup>15</sup> prescribes a deflection at the center of the plate equal to  $\frac{5h\Delta PL^4}{384EI} \approx 46 \mu\text{m}$  (where  $h$  is the depth), with  $I = \frac{b^3 h}{12}$  the moment of area. An equivalent spring stiffness per unit area  $\kappa^* = \frac{6.4 E b^3}{L^4} = 3.3 \times 10^7 \text{ N m}^{-3}$  can thus be defined, with corresponding non-dimensional value  $\kappa \approx 3$ . With the set of values reported, the plate can be considered rigid.

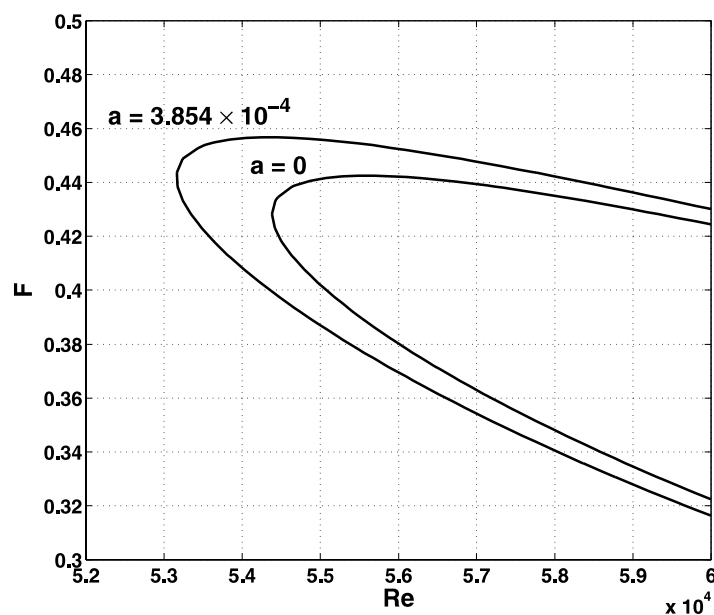


FIG. 2. Marginal stability curves for a rigid wall with  $a=0$  and for Fransson and Alfredsson's conditions, i.e.,  $a = 3.854 \times 10^{-4}$ . These neutral curves are unaffected by increasing values of  $\kappa$ .

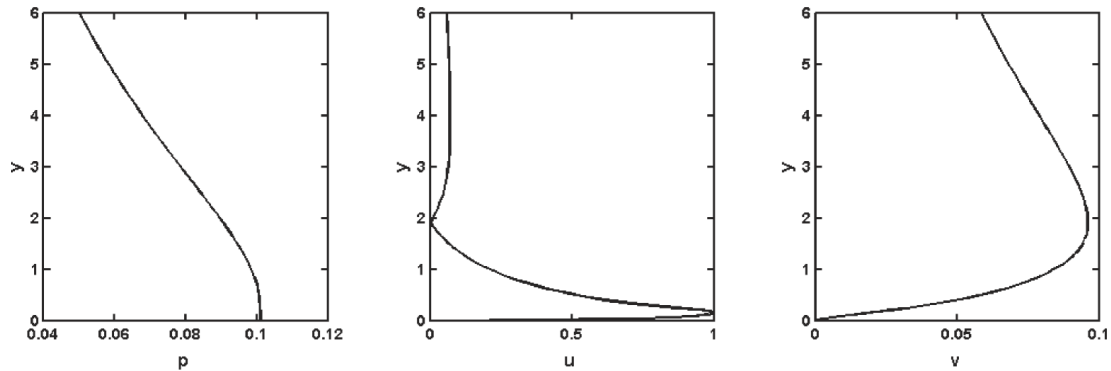


FIG. 3. Modulus of the mode shapes at the critical point ( $Re = 54\,380$ ,  $F = 0.43$ , and  $a = 0$ ).

### A. Comparison in terms of the wavenumber

The dimensionless frequency  $F$  classically used when computing boundary layer's neutral stability results is  $F = 10^6 \frac{\omega_r}{Re}$ . Marginal curves for both impermeable and permeable rigid plates are displayed in Fig. 2 to demonstrate that even a very small permeability coefficient destabilizes the boundary layer, while increasing the value of the critical frequency at the onset of TS waves. The TS mode shapes at the critical point is shown in Fig. 3.

Fransson and Alfredsson<sup>3</sup> carried out measurements in strongly stable conditions, at  $Re = 347$  and  $F = 59$ . Fig. 4 displays the real and imaginary parts of  $\alpha$  for permeability varying from 0 to 1 in the conditions of the experiments. The thin solid horizontal lines in the graph correspond to the measured values, i.e.,  $\alpha_r = 0.043$  and  $\alpha_i = 0.015$ , and are, respectively, larger and lower than the reference values obtained for  $a = 0$  by Fransson and Alfredsson (and reproduced by our calculations). The theoretical trends shown in the figure for  $a$  slightly larger than zero go in the same direction as the experiments; to render the agreement more quantitative, one may possibly need to account for the disturbance field underneath the porous plate (here neglected) or use a different model for the flow within the porous plate when the permeability is above some threshold, for example, accounting for inertia via a Forchheimer term.

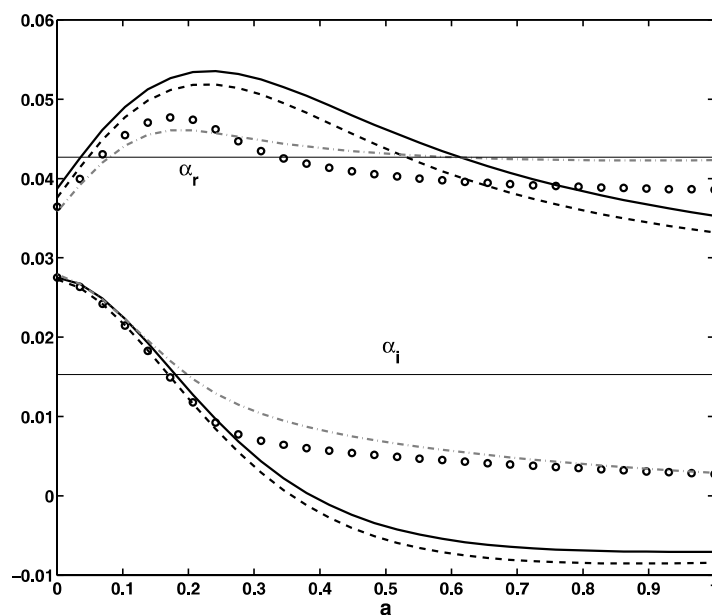


FIG. 4. Variation of real (upper curves) and imaginary (lower curves) parts of  $\alpha$  for varying wall elasticity  $E$  in the conditions of the experiments by Fransson and Alfredsson:  $Re = 347$ ,  $F = 59$ , and  $\kappa = 2.94$ . Thick solid lines: rigid wall. Dashed lines:  $E = 2 \times 10^5$  Pa. Symbols:  $E = 8 \times 10^4$  Pa. Grey dotted-dashed lines:  $E = 5 \times 10^4$  Pa. The experimental results are indicated by thin horizontal lines.

Another alternative consists in employing homogenization theory to treat the flow within the possibly anisotropic poro-elastic medium, and coupling the homogenized field with the continuum field which develops above it, by the use of some interface conditions. Whereas, the homogenized equations are reasonably well established and can be derived, for example, by the use of volume averaging<sup>16</sup> or multiple-scale theory,<sup>17</sup> doubts subsist as to the appropriate matching conditions at the interface between the two media, particularly when inertia is significant within the porous, or poroelastic, domain.

In any case, in the simplified setting employed here, we have found correct trends in comparison to the very careful experiments by Fransson and Alfredsson, and this encourages us to explore the problem further, on the basis of the current model.

## B. Influence of surface permeability

Typically, the permeability  $k_D$  is in a range from  $2 \times 10^{-17} \text{ m}^2$  (concrete) to  $10^{-6} \text{ m}^2$  (metal foams),<sup>18</sup> and depends on the porosity and the structure of the medium. With the parameters of Fransson and Alfredsson,<sup>3</sup> this translates to a range  $[2 \times 10^{-9}, 10^2]$  for the dimensionless parameter  $a$ . In the calculations to follow, we limit the upper bound to  $a = 1$  on account of Darcy's model (which is untenable when the permeability becomes too large).

The influence of  $a$  on the neutral TS curves is displayed in Fig. 5, still in the rigid-plate case. The rapid destabilization induced by increasing values of  $a$  is impressive, both in terms of the Reynolds number and in terms of the range of frequencies which can be excited. This is further elaborated in Fig. 6, which shows critical Reynolds numbers, frequencies, and wavenumbers for  $a$  between 0 and 1 (critical values are denoted with a  $c$  subscript).

For the most permeable case computed,  $Re_c$  becomes lower than 70, with a corresponding critical frequency which exceeds  $10^3$ . The behavior of the critical wavenumber (Fig. 6, right frame) is less predictable, with an initial increase for very small values of  $a$ , followed by a decrease with a minimum for  $a$  around 0.2, and a final monotonic shortening of the wavelength with the further increase of  $a$ . The values of the critical wavenumber remain, however, confined to a narrow range around  $\alpha_r = 0.15$ .

What these results clearly show is that when analyzing the stability over porous surfaces, it is fundamental to account for the effect of the permeability in the boundary conditions of the disturbance field; in most circumstances, it is not adequate to simply force zero disturbance velocity at  $y = 0$  and even relatively small values of the parameter  $a$  cause dramatic variations on the stability characteristics of the flow.

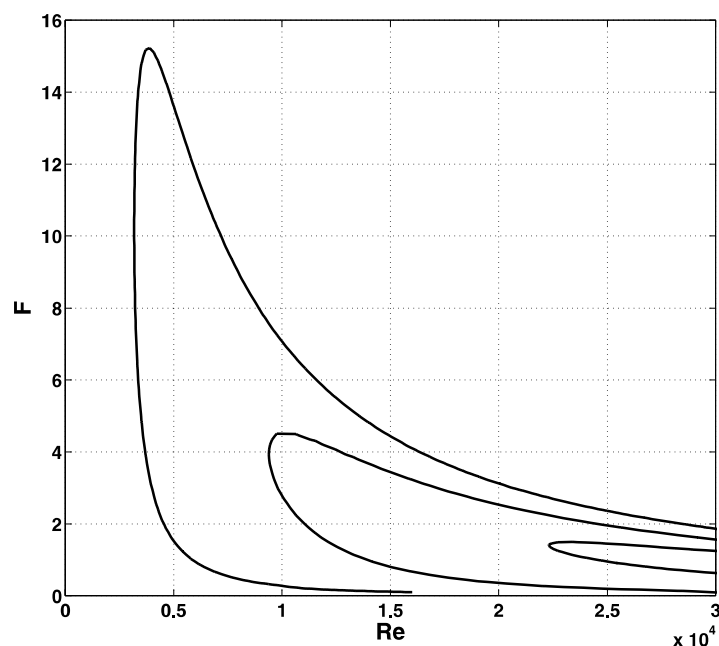


FIG. 5. Neutral curves for varying values of  $a$ ; from left to right,  $a = 0.1, 0.05$ , and  $0.02$ .

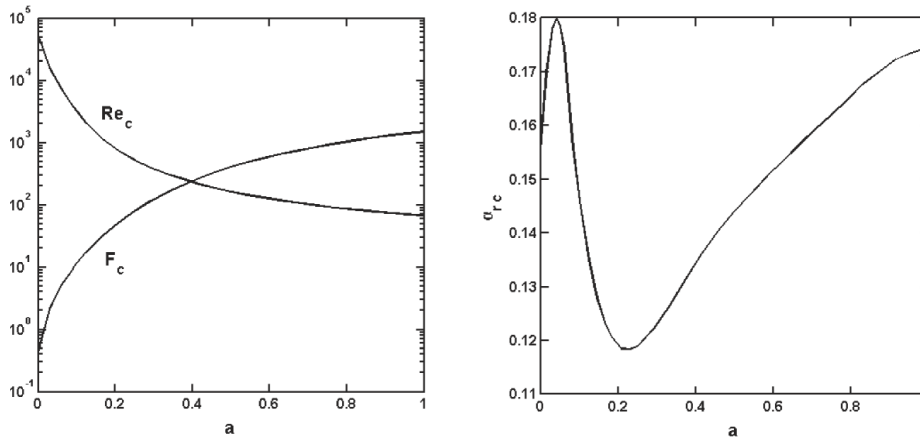


FIG. 6. Behavior of the critical Reynolds number and frequency (left frame) and of the critical wavenumber (right frame) as function of the permeability  $a$ .

#### IV. EFFECT OF PERMEABILITY AND SURFACE ELASTICITY ON TS MODES

Previous studies on the Blasius boundary layer<sup>9,19</sup> have demonstrated that decreasing the wall elasticity yields a stabilization of the TS modes. The same happens in the asymptotic suction boundary layer when  $a$  is taken to vanish, as exemplified in Fig. 7 for three values of  $E$ . Here, the Young modulus enters both the definition of  $B$  as well as  $\kappa$ , since the latter parameters depend linearly on  $E$ .

The combined effect of plate's porosity and flexibility shows the trend displayed in Fig. 8. For  $a = 0.1$ , decreasing the value of  $E$  has a mild destabilizing effect on TS waves, and this is at odds with the assumption<sup>20</sup> that class A perturbations are "stabilized by irreversible energy transfer from the fluid to the coating." For a summary of the classification of fluid-solid instabilities, we refer to Ref. 9. The unexpected destabilizing effect of compliance must be ascribed to the coupled effect of permeability and wall flexibility. There is, however, a threshold value of  $a$  below which flexibility becomes stabilizing. As an example, Fig. 8 (right) shows that the cross-over between stabilization and destabilization occurs for  $a = 0.033$ , when comparing the cases  $E \rightarrow \infty$  and  $E = 10^6$  Pa.

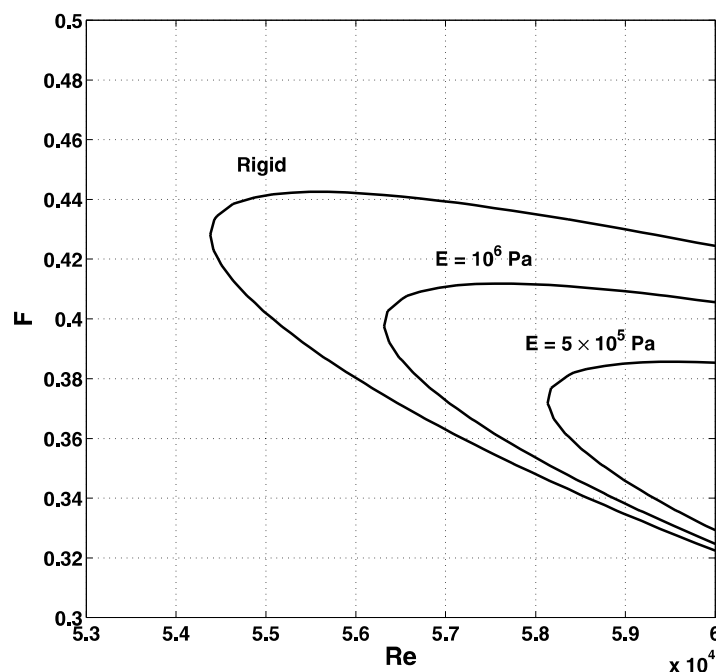


FIG. 7. Stabilization of the neutral curves for increasingly softer plates.

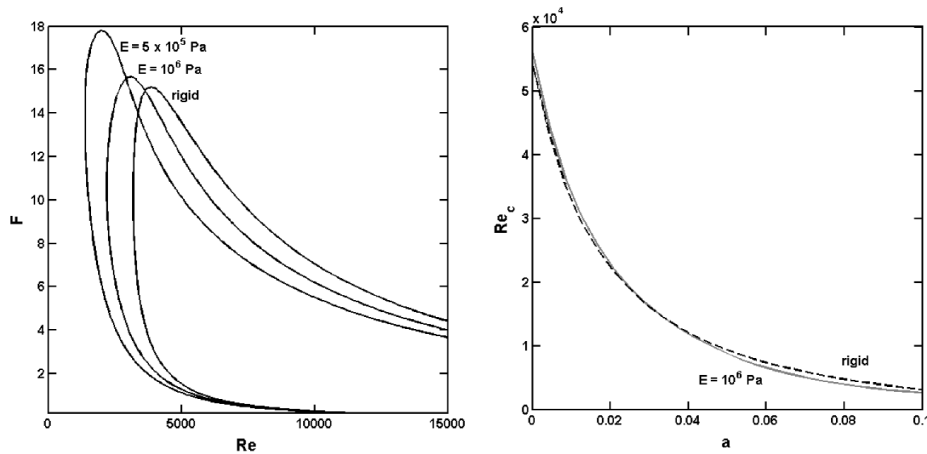


FIG. 8. Left: effect of plate's softness on the neutral stability curves for TS modes,  $a = 0.1$ . Right: combined effect of permeability and softness on TS instability threshold.

The main conclusion here is that the plate flexibility does not have a very large influence on the critical TS conditions, the major variations being associated to the permeability  $a$ . The critical Reynolds number for the onset of TS waves on a rigid plate decreases from 54 380 ( $a = 0$ ) to 3200 ( $a = 0.1$ ). On the other hand, the plate's flexibility might induce potentially dangerous surface elastic modes, addressed in Sec. V.

## V. ABSOLUTE INSTABILITY

It is interesting at this point to look at modal coalescence and search for conditions under which absolute instabilities — spreading both upstream and downstream of the point from which they originate — arise. The identification of absolutely unstable modes can be carried out on the basis of the asymptotic approach described by Briggs<sup>13</sup> and initially applied to plasma physics instabilities. This technique is thoroughly described by Schmid and Henningson.<sup>21</sup> It is on the basis of this spatio-temporal approach that Brazier-Smith and Scott<sup>22</sup> have highlighted the existence of absolutely unstable modes for the potential flow over a compliant panel, above a certain threshold velocity. Carpenter and Garrad<sup>10</sup> have put a name on such an instability, *static divergence*, suggesting that such waves were likely to be absolute over a damped, infinitely long, compliant panel. An absolute instability can also arise in the Blasius boundary layer over a compliant coating, from the coalescence between an upstream-propagating evanescent mode and a Tollmien-Schlichting wave.<sup>23,24</sup> This absolute instability has been identified as being the divergence-type mode observed by Lucey and Carpenter.<sup>25</sup>

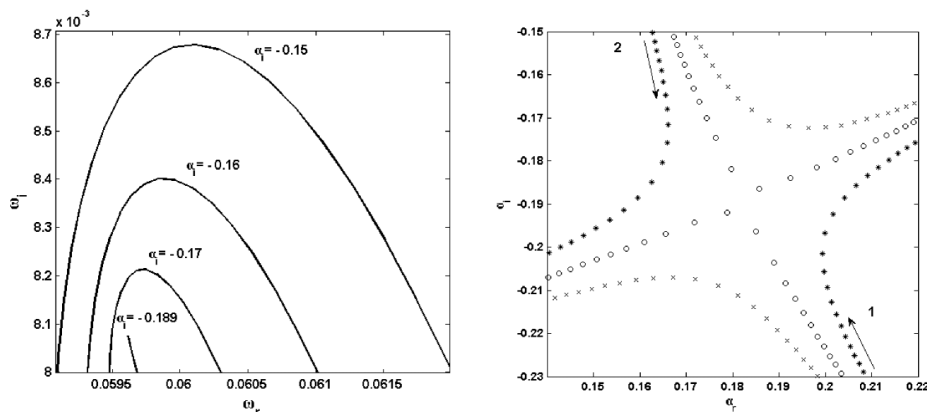


FIG. 9. Branch point (left) and corresponding saddle point in the  $\alpha$  plane upon contour deformation (right); \* :  $\omega_i = 7.98 \times 10^{-3}$ ; o :  $\omega_i = 8.08 \times 10^{-3}$ ; x :  $\omega_i = 8.18 \times 10^{-3}$  ( $E = 10$  MPa,  $Re = 28\,000$  and  $a = 0.4$ ).



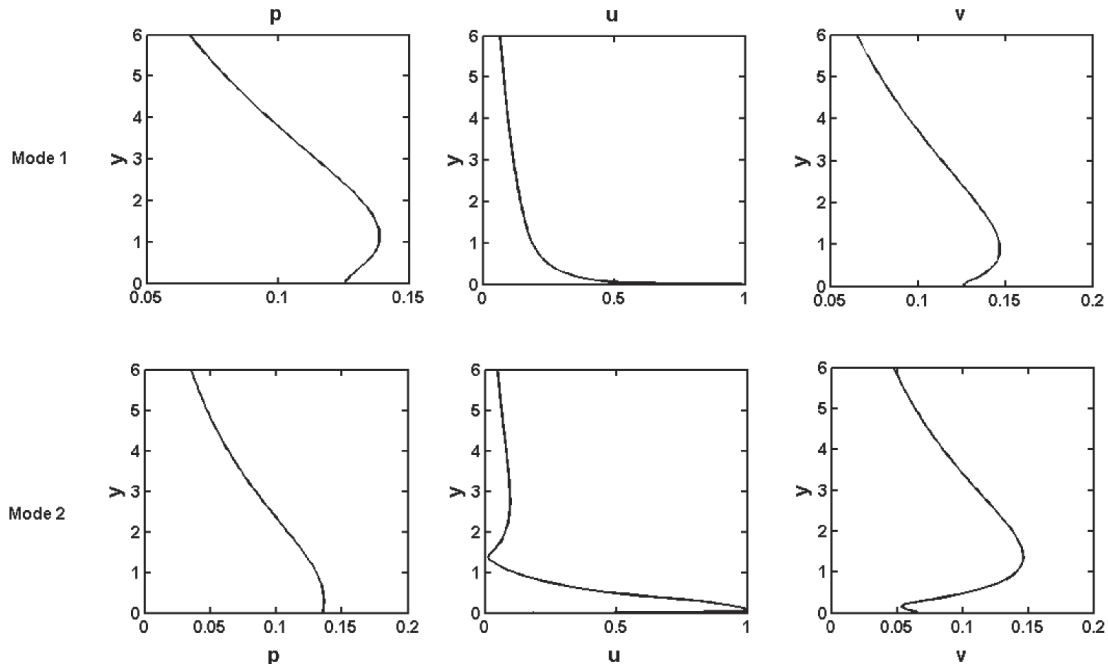


FIG. 10. Modulus of the perturbation profiles before lowering the inversion contour. Upper frame: mode 1; lower frame: mode 2 ( $E = 10$  MPa,  $Re = 28\,000$ ,  $a = 0.4$  and  $\omega = 74 \times 10^{-3} + 32.6 \times 10^{-3} i$ ).

Finally, absolute instabilities have also been detected in flows over a rotating disk with compliant coating by Cooper and Carpenter,<sup>26</sup> with suction having a stabilizing effect, as discussed by Lingwood.<sup>11</sup>

Here, we consider a free-stream speed larger than in Secs. III and IV, i.e.,  $U_\infty = 40$  m s<sup>-1</sup>, but maintain the same functional dependence of the parameters on  $E$  and  $b$ , i.e.,  $\chi$  goes like  $b$ , while  $B$  and  $\kappa$  are proportional to  $E b^3$ . We write explicitly the dependence on  $b$  to highlight the fact that the plate's thickness affects the onset of the absolute instability. We anticipate here that for  $U_\infty = 5$  m s<sup>-1</sup>, there are absolutely unstable modes only for plate's thicknesses lower than 0.1 mm, and it is precisely for this reason (e.g., to consider plates whose thickness is closer to actual values) that we have focused on a larger outer velocity.

We consider a soft, porous elastomeric plate ( $E = 10$  MPa) of thickness  $b = 2$  mm; when  $Re = 28\,000$  and  $a = 0.4$ , a branch point is found by lowering the temporal inversion contour in the Laplace plane, for  $\omega_0 = 5.96 \times 10^{-2} + 8.08 \times 10^{-3} i$ , as shown in Fig. 9 (left). This point has a singularity associated to it in the Fourier plane, when the spatial inversion contour is pinched between two spatial branches. The pinch point is found at  $\alpha_0 = 0.1808 - 0.189 i$  (Fig. 9, right frame) between a mode 1 coming from below and a mode 2 coming from above. We believe that we are in the presence of a static divergence mode.<sup>25</sup> Perturbation profiles on Fig. 10 correspond to the same conditions as the branch point, before lowering the temporal inversion contour (thus for  $\alpha_i = 0$ ). They confirm that mode 1 stems from a strongly spatially damped hydroelastic wave, named “evanescent mode” by Wiplier and Ehrenstein,<sup>24</sup> whereas mode 2 is a TS wave.

Fig. 11 demonstrates the effect of  $Re$  and  $a$  on the growth rate of the absolutely unstable mode identified. The left frame shows that the absolute instability arises fairly early ( $Re$  around 3000) and is maximally amplified near  $Re = 30\,000$ . Surprisingly, the imaginary part of  $\omega_0$  decreases for larger values of the Reynolds numbers with the mode becoming convective at very large values of  $Re$ . When the plate is rendered more rigid ( $E = 30$  MPa), the range of  $Re$  for which an absolutely unstable mode appears is reduced, and the absolute instability appears very early (in  $Re$  terms). Similar results have been reported by Wiplier and Ehrenstein<sup>24</sup> in a Blasius boundary layer, with the viscous substrate playing a damping role in their case.

The influence of the plate permeability is rendered in the right frame of Fig. 11. The first observation is that the absolutely unstable mode exists also for  $a = 0$ . Previous authors (see, for example, Landahl<sup>27</sup> or Carpenter and Garrad<sup>10</sup>) have noted that damping is necessary for the onset of this

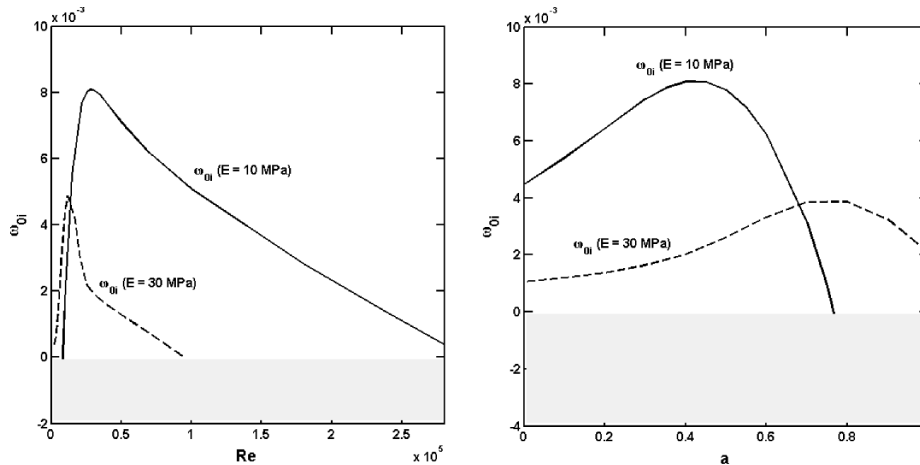


FIG. 11. Evolution of the growth rate of the absolute instability mode as function of  $Re$  for  $a = 0.4$  (left frame) and as function of  $a$  ( $Re = 28\,000$ ), for soft and rigid plates.

mode on infinitely long wall, while edge conditions can play the same role on finite surfaces. Lucey and Carpenter<sup>25</sup> suggest that both damping and edge effects can be liable to break the balance between hydrodynamic stiffness and restoring forces; here, we see that suction is sufficient to play this destabilizing role, in the absence of damping. Furthermore, for both the softer and the more rigid plate, an increasing permeability has initially the effect of enhancing the absolute instability, before a subsequent stabilization. Thus, the porous wall plays a role analogous to dissipation: a small amount of it slows the propagation of surface waves and favours the transfer of energy from the fluid to the wall. Conversely, a strong permeability has a damping effect and inhibits the growth of the static divergence mode.<sup>25</sup>

## VI. CONCLUSIONS

The motion of fluid over and through walls which are both permeable and compliant can be found in nature, i.e., canopy flows, fluid going through the lungs or in the inner ears (with ciliated surfaces), motion through the feathers of birds' wings, as well as in technological applications, since suction is, for example, being tested as a mean of flow control through wings and nacelles of airplanes, both exhibiting compliance to some degree. It is thus important to understand the combined effect of surface suction and flexibility on the onset and growth of instability modes. The present contribution represents a step in this direction, albeit in the simplified setting of the ASBL.

Boundary conditions at the wall have been tested, which take into account the plate's permeability on the linear disturbance field; permeability is quantified by a parameter,  $a$ , which is the product of the Darcy number ( $Da = k_D/b^2$ ), the Reynolds number,  $Re$ , and the ratio between the plate's thickness,  $b$ , and the boundary layer displacement thickness,  $\delta^*$ . The permeability coefficient  $a$  significantly destabilizes TS waves; conversely, elasticity of the wall plays a minor effect, i.e., mildly destabilizing for small values of  $a$  and mildly stabilizing when  $a$  overcomes a certain threshold, function of  $E$ .

The possible presence of absolutely unstable modes has also been addressed here; they arise from the coalescence of an evanescent, hydroelastic mode and a TS wave, giving rise to a quasi-static divergence instability, which can be very important over a wide range of  $Re$  and  $a$ . This mode is enhanced by the plate becoming softer. Previous studies<sup>25,27,28</sup> have suggested the need for dissipation in the wall for the appearance of the static divergence mode on infinite flexible walls. Here we have shown that wall-dissipation is probably not necessary, and that suction through the wall is sufficient for the static divergence instability to emerge.

Possible extensions of this work may be envisioned by considering an anisotropic bounding surface, eventually with flow through it also along the  $x$ -direction, for the  $u = 0$  condition at  $y = 0$  (in the rigid case) to be relaxed.

## ACKNOWLEDGMENTS

This work started thanks to a Vinci mobility grant awarded to the two senior authors by the “Università Italo-Francese” (Project No. C1-28). A.B. further acknowledges the partial financial support awarded from the EU to Wolf Dynamics through the PelSkin project (Grant No. ACP2-GA-2013-334954-PEL-SKIN) and the support from the PRIN 2012 Project No. D38C1300061000 funded by the Italian Ministry of Education.

- <sup>1</sup> R. D. Joslin, “Aircraft laminar flow control,” *Annu. Rev. Fluid Mech.* **30**, 1–29 (1998).
- <sup>2</sup> L. M. Hocking, “Nonlinear instability of the asymptotic suction velocity profile,” *Q. J. Mech. Appl. Math.* **28**, 341–353 (1975).
- <sup>3</sup> J. H. M. Fransson and P. H. Alfredsson, “On the disturbance growth in an asymptotic suction boundary layer,” *J. Fluid Mech.* **482**, 51–90 (2003).
- <sup>4</sup> W. Pfenniger and E. Groth, “Low drag boundary layer suction experiments in flight on a wing glove of an F94A airplane with suction through a large number of fine slots,” in *Boundary Layer and Flow Control: Its Principles and Applications* Vol. II (Pergamon Press, Oxford, 1961), pp. 981–999.
- <sup>5</sup> G. A. Reynolds and W. S. Saric, “Experiments on the stability of the flat-plate boundary layer with suction,” *AIAA J.* **24**, 202–207 (1986).
- <sup>6</sup> D. G. MacManus and J. A. Eaton, “Flow physics of discrete boundary layer suction measurements and predictions,” *J. Fluid Mech.* **417**, 47–75 (2000).
- <sup>7</sup> N. Gregory, “Research on suction surfaces for laminar flow,” in *Boundary Layer and Flow Control: Its Principles and Applications* Vol. II (Pergamon Press, Oxford, 1961), pp. 924–957.
- <sup>8</sup> J. H. M. Fransson, “Investigations of the asymptotic suction boundary layer,” TRITA-MEK Tech. Rep. 2001:11. Licentiate Thesis, Department of Mechanics, KTH, SE-100 44 Stockholm, Sweden, 2001.
- <sup>9</sup> F. Pluinage, A. Kourta, and A. Bottaro, “Instabilities in the boundary layer over a permeable, compliant wall,” *Phys. Fluids* **26**, 084103 (2014).
- <sup>10</sup> P. W. Carpenter and A. D. Garrad, “The hydrodynamic stability of flow over Kramer-type compliant surfaces. Part 2. Flow-induced surface instabilities,” *J. Fluid Mech.* **170**, 199–232 (1986).
- <sup>11</sup> R. J. Lingwood, “On the effects of suction and injection on the absolute instability of the rotating-disk boundary layer,” *Phys. Fluids* **9**(5), 1317–1328 (1997).
- <sup>12</sup> A. A. Griffith and F. W. Meredith, “The possible improvement in aircraft performance due to boundary layer suction,” Technical Report 2315, Report of the Aeronautical Research Council, 1936.
- <sup>13</sup> R. J. Briggs, *Electron-Stream Interaction with Plasmas* (MIT Press, Cambridge, MA, 1964).
- <sup>14</sup> C. Gustavsson, “Development of three-dimensional disturbances in boundary layers with suction,” Master’s thesis (Luleå University of Technology, Luleå, Sweden, 2000).
- <sup>15</sup> L. Chevalier, *Mécanique des Systèmes et des Milieux Déformables* (Ellipses, 2004).
- <sup>16</sup> S. Whitaker, *The Method of Volume Averaging*, Theory and Applications of Transport in Porous Media (Springer, 1999).
- <sup>17</sup> C. C. Mei and B. Vernescu, *Homogenization Methods for Multiscale Mechanics* (World Scientific, 2010).
- <sup>18</sup> M. Innocentini, P. Sepulveda, and F. Ortega, in *Cellular Ceramics: Structure, Manufacturing, Properties and Applications*, edited by M. Scheffler and P. Colombo (Wiley-VCH Verlag GmbH, Weinheim, Germany, 2005), pp. 313–341.
- <sup>19</sup> P. W. Carpenter and A. D. Garrad, “The hydrodynamic stability of flow over Kramer-type compliant surfaces. Part 1. Tollmien-Schlichting instabilities,” *J. Fluid Mech.* **155**, 465–510 (1985).
- <sup>20</sup> M. Gad-el-Hak, “Compliant coatings: A decade of progress,” *Appl. Mech. Rev.* **49**(10), S147–S157 (1996).
- <sup>21</sup> P. J. Schmid and D. S. Henningson, *Stability and Transition in Shear Flows*, Applied Mathematical Sciences Vol. 142 (Springer, New York, 2001).
- <sup>22</sup> P. R. Brazier-Smith and J. F. Scott, “Stability of fluid flow in the presence of a compliant surface,” *Wave Motion* **6**(6), 547–560 (1984).
- <sup>23</sup> K. S. Yeo, B. C. Khoo, and H. Z. Zhao, “The absolute instability of boundary-layer flow over viscoelastic walls,” *Theor. Comput. Fluid Dyn.* **8**(4), 237–252 (1996).
- <sup>24</sup> O. Wiplier and U. Ehrenstein, “On the absolute instability in a boundary-layer flow with compliant coatings,” *Eur. J. Mech., B: Fluids* **20**, 127–144 (2001).
- <sup>25</sup> A. D. Lucey and P. W. Carpenter, “A numerical simulation of the interaction of a compliant wall and an inviscid flow,” *J. Fluid Mech.* **234**, 121–146 (1992).
- <sup>26</sup> A. J. Cooper and P. W. Carpenter, “The stability of rotating-disc boundary-layer flow over a compliant wall. Part 2. Absolute instability,” *J. Fluid Mech.* **350**, 261–270 (1997).
- <sup>27</sup> M. T. Landahl, “On the stability of a laminar incompressible boundary over a flexible surface,” *J. Fluid Mech.* **13**, 609–632 (1962).
- <sup>28</sup> C. Davies and P. W. Carpenter, “Instabilities in a plane channel flow between compliant walls,” *J. Fluid Mech.* **352**, 205–243 (1997).